



**Queensland University of Technology**  
Brisbane Australia

This is the author's version of a work that was submitted/accepted for publication in the following source:

Bahfenne, Silmarilly, Rintoul, Llewellyn, Langhof, Jorgen, & Frost, Ray L. (2012) Single crystal raman spectroscopy of natural paulmooreite  $Pb_2As_2O_5$  and in comparison with the synthesised analogue. *American Mineralogist*, 97(1), pp. 143-149.

This file was downloaded from: <http://eprints.qut.edu.au/48072/>

© Copyright 2012 American Mineralogical society

**Notice:** *Changes introduced as a result of publishing processes such as copy-editing and formatting may not be reflected in this document. For a definitive version of this work, please refer to the published source:*

1 **REVISION 1**

2

3 **Single Crystal Raman Spectroscopy of Natural Paulmooreite  $\text{Pb}_2\text{As}_2\text{O}_5$  and**  
4 **in Comparison with the Synthesised Analogue**

5

6 **SILMARILLY BAHFENNE<sup>1</sup>, LLEW RINTOUL<sup>1</sup>, JÖRGEN LANGHOF,<sup>2</sup> RAY L. FROST<sup>1</sup> •**

7

8 <sup>1</sup>Chemistry Discipline, Faculty of Science and Technology, Queensland University of  
9 Technology, GPO Box 2434, Brisbane Queensland 4001, Australia.

10

11 <sup>2</sup> Curator of minerals, Department of Mineralogy, Swedish Museum of Natural History, Box  
12 50007, SE-104 05 Stockholm

13

14

15 **ABSTRACT**

16

17 The single crystal Raman spectra of natural mineral paulmooreite  $\text{Pb}_2\text{As}_2\text{O}_5$  from the  
18 Långban locality, Filipstad district, Värmland province, Sweden are presented for the  
19 first time. It is a monoclinic mineral containing an isolated  $[\text{As}_2\text{O}_5]^{4-}$ . Depolarised and  
20 single crystal spectra of the natural and synthetic sample compare favorably and are  
21 characterized by strong bands around 186 and 140  $\text{cm}^{-1}$  and three medium bands at 800 –  
22 700  $\text{cm}^{-1}$ . Band assignments were made based on band symmetry and spectral  
23 comparison between experimental band positions and those resulting from Hartree-Fock

---

• Author to whom correspondence should be addressed (r.frost@qut.edu.au)

24 calculation of an isolated  $[\text{As}_2\text{O}_5]^{4-}$  ion. Spectral comparison was also made with lead  
25 arsenites such as synthetic  $\text{PbAs}_2\text{O}_4$  and  $\text{Pb}_2(\text{AsO}_2)_3\text{Cl}$  and natural finnemanite in order  
26 to determine the contribution of the terminal and bridging O in paulmooreite. Bands at  
27  $760 - 733 \text{ cm}^{-1}$  were assigned to terminal As-O vibrations, whereas stretches of the  
28 bridging O occur at  $562$  and  $503 \text{ cm}^{-1}$ . The single crystal spectra showed good mode  
29 separation, allowing bands to be assigned a symmetry species of  $A_g$  or  $B_g$ .

30

31 **KEYWORDS:** paulmooreite, finnemanite, single crystal Raman spectroscopy;  $\text{PbAs}_2\text{O}_4$ ;  
32  $\text{Pb}_2(\text{AsO}_2)_3\text{Cl}$

33

34

## 35 INTRODUCTION

36 Paulmooreite is a lead arsenite mineral containing dimeric  $[\text{As}_2\text{O}_5]^{4-}$  units, which was first  
37 announced as a new mineral by Dunn et al. (1979). The natural paulmooreite sample was  
38 kindly supplied by the Swedish Museum of Natural History (specimen number  
39 NRM532109). In preparing a synthetic analogue of paulmooreite, hydrothermal and wet  
40 synthetic methods were explored including the method given by Pertlik (1988) who reported  
41 the presence of  $\text{Pb}_2\text{As}_2\text{O}_5$  among the products of the hydrothermal synthesis of  $\text{Pb}_2(\text{AsO}_2)_3\text{Cl}$ .  
42 The details of the different synthetic routes will be discussed in the Experimental section.

43

44 No other pyroarsenite compounds had been studied to date with Raman spectroscopy apart  
45 from the theoretical study by Tossell (1997). Vajdakite,  $[(\text{MoO}_2)_2(\text{H}_2\text{O})_2\text{As}_2\text{O}_5]\cdot\text{H}_2\text{O}$ , also  
46 possesses  $[\text{As}_2\text{O}_5]^{4-}$  units (Ondrus *et al.*, 2002) and had been studied previously with Raman  
47 spectroscopy (Cejka *et al.*, 2010). However the presence of two inequivalent  $\text{MoO}_5(\text{H}_2\text{O})$   
48 units makes it difficult to identify and assign the vibrations of the unit since there may be

49 some coincidence of the bands. A study on some pyroantimonite compounds had been  
50 published (Hirschle and Röhr, 2000). In  $\text{Cs}_4\text{Sb}_2\text{O}_5$  the  $\text{SbO}_3$  pyramids of the  $[\text{Sb}_2\text{O}_5]^{4-}$  unit  
51 have the  $180^\circ$  orientation. Its Raman spectrum is similar to that of paulmooreite in the 800 –  
52  $600\text{ cm}^{-1}$  region; a strong band at 700, a medium band at 650, and a weak band at  $615\text{ cm}^{-1}$   
53 (Fig. 4 of Hirschle and Röhr, 2000). The first two bands were assigned to terminal Sb-O and  
54 the last to bridging Sb-O vibrations. This assignment agrees broadly with assignments made  
55 in the present study.

56

57 To aid the determination of the contribution of the diarsenite unit to the vibrational spectra,  
58 the Raman spectrum of an isolated  $[\text{As}_2\text{O}_5]^{4-}$  ion was calculated using Hartree-Fock methods.  
59 Furthermore to determine the contribution of the bridging and terminal As-O atoms the  
60 spectra of  $\text{Pb}_2\text{As}_2\text{O}_5$  was compared with related synthetic compounds  $\text{PbAs}_2\text{O}_4$  and  
61  $\text{Pb}_2(\text{AsO}_2)_3\text{Cl}$  and natural finnemanite  $\text{Pb}_5(\text{AsO}_3)_3\text{Cl}$ . The vibrational spectra of paulmooreite  
62 and the above compounds have not been previously published. This study presents the single  
63 crystal data for natural and synthetic paulmooreite and makes band assignments according to  
64 symmetry and type.

65

## 66 **Experimental**

### 67 *Minerals*

68 Single crystals of paulmooreite and finnemanite were supplied by the Swedish Museum of Natural History of  
69 specimen numbers NRM532109 and NRM883736 respectively. The specimen originated from the Långban  
70 locality, Filipstad district, Värmland province, Sweden. The mineral is colourless to pale yellow. (see  
71 <http://www.mindat.org/min-3135.html>).

72

### 73 *Synthesis of the mineral paulmooreite*

74 Pertlik (1988) reported the hydrothermal synthesis of  $\text{Pb}_2(\text{AsO}_2)_3\text{Cl}$ . Three types of reactions were performed.  
75 The first entailed mixing  $\text{PbCl}_2$  and  $\text{PbO}$  in a 1:10 weight ratio and  $\text{As}_2\text{O}_3$  in 1M acetic acid with varying  
76 conditions (P1 - 150°C for 4 days, P2 - 50°C for 4 days, P3 - 150°C for 10 days, and P4 - 60°C for 7 days). In  
77 the second set of reactions  $\text{PbO}$  and  $\text{As}_2\text{O}_3$  were hydrothermally reacted in a mole ratio of 2:1. In all cases 1M  
78 acetic acid was used as solvent unless indicated. The conditions were: H1- 150°C for 10 days using 1M acetic  
79 acid, H2- 210°C for 4 days using 1M acetic acid, H3- 60°C for 7 days using 1M acetic acid purged with  $\text{N}_2$ , H4  
80 - 150°C for 2 days using 1M acetic acid purged with  $\text{N}_2$ , and H5 - 150°C for 2 days using water purged with  
81  $\text{N}_2$ . The third set were wet synthesis methods in which,  $\text{NaOH}$  and  $\text{As}_2\text{O}_3$  were mixed in a ratio of 4:1 to give  
82 one mole of  $\text{Na}_4\text{As}_2\text{O}_5$ , which was then mixed with two moles of  $\text{Pb}(\text{NO}_3)_2$ . The precipitate and mother liquor  
83 were aged for 7 days at W1 - room temperature, W2 - 40°C, and W3 - 60°C.

84

### 85 *Raman Microscopy*

86 A natural crystal of paulmooreite was placed on the corner of a cube and aligned parallel to the sides of the  
87 cube. It was assumed that the crystal laid on its perfect (001) cleavage plane. In the plane of the crystal, the  
88 long axis corresponded to the  $b$  axis, and the  $a$  axis was at right angles to the long axis. Crystals of  
89 paulmooreite are tabular on [100] or [001], leading to easier collection of spectra on these faces and avoiding  
90 birefringence. The synthetic crystal was not oriented due to its small size.

91

92 The instrument used was a Renishaw 1000 Raman microscope system, which also includes a monochromator, a  
93 Rayleigh filter system and a CCD detector coupled to an Olympus BHSM microscope equipped with 10x, and  
94 50x objectives. The Raman spectra were excited by a Spectra-Physics model 127 He-Ne laser producing plane  
95 polarised light at 633 nm and collected at a resolution of better than  $4 \text{ cm}^{-1}$  and a precision of  $\pm 1 \text{ cm}^{-1}$  in the  
96 range between 120 and  $4000 \text{ cm}^{-1}$ . Repeated acquisitions on the crystals using the highest magnification (50x)  
97 were accumulated to improve the signal-to-noise ratio in the spectra. The instrument was calibrated prior to use  
98 using the  $520.5 \text{ cm}^{-1}$  line of a silicon wafer. In the normal course of spectral accumulation 20 scans were  
99 accumulated at 20 s time intervals.

100

101 Spectral manipulation such as baseline correction/adjustment was performed using the GRAMS software  
102 package (Galactic Industries Corporation, NH, USA). Band component analysis was undertaken using the  
103 Jandel 'Peakfit' software package (version 1) that enabled the type of fitting function to be selected and allows

104 specific parameters to be fixed or varied accordingly. Band fitting was done using a Lorentzian-Gaussian cross-  
105 product function with the minimum number of component bands used for the fitting process. The Lorentzian-  
106 Gaussian ratio was maintained at values greater than 0.7 and fitting was undertaken until reproducible results  
107 were obtained with squared correlations of  $R^2$  greater than 0.995.

108

### 109 *Hartree-Fock Calculations*

110 Calculations were performed using the Gaussian 03 program (Frisch *et al.*, 2004) and the GaussView 4.0  
111 (Gaussian, Inc., Wallingford, CT) front end, running on an SGI Origin 3000 supercomputer. The wavenumber  
112 of the fundamental modes were calculated using Hartree-Fock (HF) with B3-LYP method and a 6-31G(d) basis  
113 set for O atoms and Lan12dz for As. A scaling factor of 0.972 was applied. Raman intensities were calculated  
114 from the Gaussian activities based on 633 nm excitation.

115

## 116 **DESCRIPTION OF CRYSTAL STRUCTURE**

117

118 Paulmooreite structure was refined by Moore *et al.* (1980) who placed it in the monoclinic  
119 space group  $P2_1/a$  ( $C_{2h}^5$ ),  $a = 13.584$ ,  $b = 5.650$ ,  $c = 8.551$  Å, and  $Z = 4$ . It belongs to a small  
120 group of diarsenite minerals consisting of vajdakite  $[(MoO_2)_2(H_2O)_2As_2O_5] \cdot H_2O$  (Ondrus *et*  
121 *al.* 2002) and gebhardite  $Pb_8(As_2O_5)_2OCl_6$  (Klaska and Gebert, 1982); the dimeric unit in  
122 each mineral differing by the orientation of one trigonal pyramid to the other. In  
123 paulmooreite, the triangular bases of the dimer are oriented nearly normal to each other  
124 (Moore *et al.* 1980).

125

126 Paulmooreite is monoclinic with space group  $P2_1/a$  ( $C_{2h}^5$ ) and four formula units (Moore *et*  
127 *al.*, 1980). The crystal cell dimensions are  $a = 13.584$ ,  $b = 5.650$ ,  $c = 8.551$  Å. Two non-  
128 equivalent  $As^{3+}$  atoms are connected through a common O atom and two other O atoms each,  
129 forming a dimeric  $[As^{3+}_2O_5]^{4-}$  unit. Each  $AsO_3$  pyramid in the  $[As_2O_5]^{4-}$  unit may be oriented  
130 in number of different ways with respect to the other; parallel orientation (Fig.1a),  $90^\circ$

131 orientation, and 180° orientation. In paulmooreite the dimers have approximately 90°  
132 orientation (Fig.1b), where one AsO<sub>3</sub> pyramid is rotated 90° from the ideal parallel  
133 orientation. There are also two inequivalent Pb<sup>2+</sup> atoms in distorted tetragonal pyramidal  
134 geometry. The symmetry of the AsO<sub>3</sub> pyramids is reduced to C<sub>1</sub> from the ideal trigonal  
135 pyramid (C<sub>3v</sub>) symmetry. The bridging O<sub>(3)</sub> atom has longer bond lengths to As<sub>(1)</sub> and As<sub>(2)</sub>  
136 than the terminal O atoms. As<sub>(1)</sub>-O<sub>(3)</sub> and As<sub>(2)</sub>-O<sub>(3)</sub> bond lengths are 1.826 and 1.842 Å,  
137 respectively. The bond lengths of the terminal O atoms belonging to As<sub>(1)</sub> are 1.747 and  
138 1.750 Å, and those belonging to As<sub>(2)</sub> are 1.733 and 1.772 Å.

139

140 **Insert Figures 1a and 1b here**

141

## 142 **RESULTS**

### 143 *X-ray Diffraction*

144

145 The first set of reactions had resulted in the formation of PbAs<sub>2</sub>O<sub>4</sub> and Pb<sub>2</sub>(AsO<sub>2</sub>)<sub>3</sub>Cl instead  
146 of Pb<sub>2</sub>As<sub>2</sub>O<sub>5</sub> as reported by Pertlik [5]. Fig. 2 shows the XRD pattern of the product of P3.

147 The reactions H1 and H2 gave hydroxymimetite Pb<sub>5</sub>(AsO<sub>4</sub>)<sub>3</sub>OH (Fig. 3). In an attempt to  
148 minimise oxidation of As<sup>3+</sup>, subsequent reactions used N<sub>2</sub>-purged solvents. Only  
149 PbAs<sub>2</sub>O<sub>4</sub> resulted from the reaction H3, whereas H4 and H5 gave Pb<sub>2</sub>As<sub>2</sub>O<sub>5</sub> and PbAs<sub>2</sub>O<sub>4</sub> at  
150 ratios of 70:30 and 50:50 respectively. Wet synthesis reactions W1 and W2 gave  
151 Pb<sub>2</sub>As<sub>2</sub>O<sub>5</sub> as the major constituent. The product of W3 also shows Pb<sub>2</sub>As<sub>2</sub>O<sub>5</sub>; however  
152 PbAs<sub>2</sub>O<sub>6</sub> is also detected among other products that could not be identified.

153

154

155

156 **Insert Figure 2 and 3 here**

157

158

159 ***Scanning Electron Microscopy***

160 The SEM micrographs of  $\text{Pb}_2\text{As}_2\text{O}_5$  synthesised by reactions W1 and W2 are shown in Fig. 4

161 a, b. The product of W1 appears to have three different morphologies. There are aggregates

162 of small fibrous particles, between which are interspersed thin plates of about 10 – 20

163 microns arranged in a pine-needle formation. A significant amount of the crystals takes the

164 form of flat plates of about 20 – 100 microns. The product of W2 appears uniform in

165 morphology and very similar to the fibrous particles in W1 except that in this case they form

166 spheres.

167

168 **Insert Figures 4a and 4b here**

169

170 ***Factor Group Analysis (FGA)***

171 The unit cell of paulmooreite is the primitive unit cell and it contains four formula units.

172 Thus a primitive unit cell contains 36 atoms. The number of allowable modes is 105

173 consisting of  $27A_g$ ,  $27B_g$ ,  $26A_u$ , and  $25B_u$ . The form of the polarisability tensor for  $C_{2h}$

174 crystals dictates that  $A_g$  modes are observed in the aa, bb, cc, and ac orientations and  $B_g$

175 modes in the ab and bc orientations. The isolated  $[\text{As}_2\text{O}_5]^{4-}$  ion with the pyramidal bases in a

176 parallel orientation has  $C_{2v}$  symmetry and 15 normal modes of vibration consisting of  $5A_1 +$

177  $3A_2 + 3B_1 + 4B_2$ . On a  $C_1$  site, such as the case with paulmooreite, each of the above modes

178 turns into an A mode, and each A mode splits into  $A_g$ ,  $B_g$ ,  $A_u$  and  $B_u$  in a  $C_{2h}$  crystal.

179

180



181 ***Raman Spectroscopy***

182 Paulmooreite is biaxially positive with a birefringence of about 0.110. The optical direction  
183 which coincides with the *b* axis is Y, meaning that light travelling along the *b* axis will not  
184 encounter circular sections and will therefore experience birefringence. Crystals of  
185 paulmooreite are tabular on [100] or [001], leading to easier collection of spectra on these  
186 faces and avoiding birefringence.

187

188 Fig. 5 shows spectra collected on the *a* and *c* faces of natural paulmooreite and a spectrum of  
189 the product of reaction W2. All three spectra compare favourably, with minor differences.  
190 The strongest band in all three spectra occurs at  $186\text{ cm}^{-1}$ , followed in intensity by a band  
191 near  $140\text{ cm}^{-1}$ , and a group of bands in the  $800 - 600\text{ cm}^{-1}$  region. The synthetic spectrum  
192 shows bands at  $637$  and  $598\text{ cm}^{-1}$  which were not observed in the natural spectra. A strong  
193 band near  $140\text{ cm}^{-1}$  seems to be broader and may consist of two bands in the synthetic  
194 spectrum, and sharper in the natural spectra. Whether or not the above bands are 'real' will  
195 be explored in later sections based on the single crystal data.

196

197 The single crystal data of natural paulmooreite are presented in Figs. 6, 9 and 10. Two non-  
198 polarised spectra collected on the *a* and *c* faces are shown, along with the parallel and  
199 perpendicular spectra of each face. Single crystal spectra of synthetic paulmooreite are  
200 shown in Figs. 7 and 8. A non-polarised, parallel, and perpendicular spectrum was collected  
201 on the tabular face of the crystal.

202

203 A group of bands in the  $800 - 700\text{ cm}^{-1}$  region (Fig. 6) appears to consist of two  $A_g$  and  $B_g$   
204 bands, whereas the group of bands in the  $700 - 600\text{ cm}^{-1}$  region (Fig. 7) consists of three  
205 bands instead of the four observed in the non-polarised spectrum of synthetic paulmooreite

206 (Figs. 7 and 9). The assignment of the bands around 640 and 598  $\text{cm}^{-1}$  in the synthetic  
207 spectrum is uncertain since neither the parallel nor perpendicular spectra show these bands.  
208 However the natural non-polarised spectrum collected on the *a*-face and the ABCA spectrum  
209 show the 640  $\text{cm}^{-1}$  band clearly defined and thus assigned to  $B_g$  symmetry. The weak band at  
210 598  $\text{cm}^{-1}$  is only observed in the Raman spectra of products of reactions H4, W2 and W3 and  
211 hence may be due to edge effect, resulting from the small crystal domain size. The same  
212 applies to the very weak band just above 350  $\text{cm}^{-1}$ . A band at 560  $\text{cm}^{-1}$  is detected only in the  
213 spectra collected on the *a*-face. Although it is weak, it is clearly defined in the depolarised *a*-  
214 face and ABCA spectra and was determined to be of  $B_g$  symmetry. The presence of two  
215 components in the band near 140  $\text{cm}^{-1}$  as suggested by the broadness of this band in the  
216 depolarised synthetic spectrum is confirmed by the presence of the weak  $B_g$  band just above  
217 140 and the strong  $A_g$  band just below 140  $\text{cm}^{-1}$ . The complete band symmetry assignments  
218 are presented in Table 2.

219

220 **Insert Figures 5 to 10 here**

221

## 222 *Discussion*

223 Out of the 54 allowable Raman modes of paulmooreite 27 modes were observed consisting of  
224  $11A_g$  and  $16B_g$  modes. Two types of As-O stretches can be expected corresponding to  
225 terminal and bridging As-O atoms. The symmetry of each  $\text{AsO}_3$  group in the  $[\text{As}_2\text{O}_5]^{4-}$  ion is  
226 reduced from the ideal trigonal pyramid ( $C_{3v}$ ) symmetry to  $C_1$ . In an isolated  $[\text{As}_2\text{O}_5]^{4-}$  ion  
227 with parallel orientation (thus having  $C_{2v}$  symmetry), stretches of the bridging O gives  $A_1$   
228 (symmetric) and  $B_2$  (antisymmetric) modes while its symmetric deformation gives  $A_1$  mode.  
229 Stretches of the terminal O atoms should give  $A_1$ ,  $A_2$ ,  $B_1$ , and  $B_2$  modes. If the ion occupies a  
230  $C_1$  site such as the case with paulmooreite each vibration will turn into a vibration of A

231 symmetry, each of which will split into an  $A_g$  and  $B_g$  component in a  $C_{2h}$  crystal. The low  
232 symmetry in paulmooreite limits the value of factor group analysis in band assignment,  
233 therefore to aid in the task of assigning bridging and terminal O vibrations the spectra of  
234 paulmooreite are compared with the HF calculated Raman spectrum and the spectra of a  
235 number of lead arsenite compounds containing polymeric and discrete  $AsO_3$  groups.

236

237 *Insert Table 1 here*

238

239 Spectra of natural paulmooreite collected on the  $a$  and  $c$  faces of the crystal are shown in Fig.  
240 14 along with  $PbAs_2O_4$  resulting from reaction H5,  $Pb_2(AsO_2)_3Cl$  from reaction P3, natural  
241 finnemanite ( $Pb_5(AsO_3)_3Cl$ ), and the HF calculated Raman spectrum of an isolated  $[As_2O_5]^{4-}$   
242 with parallel orientation ( $C_{2v}$  symmetry).

243

244  $PbAs_2O_4$  and  $Pb_2(AsO_2)_3Cl$  consist of polymerised  $AsO_3$  groups arranged into  $As_4O_8$  rings  
245 (Dinterer *et al.*, 1988) and open-branched single chains (Pertlik, 1988), respectively.  
246 Finnemanite, on the other hand, possesses isolated  $AsO_3$  pyramids (Pertlik and Effenberger,  
247 1979).

248

249 *Insert Figure 11 here*

250

251 All of the compounds show two or three bands in the  $850 - 700\text{ cm}^{-1}$  region. A band at  $734$   
252  $\text{cm}^{-1}$  ( $\nu_1$ ) is the most intense in the finnemanite spectrum, with the other bands down to  $200$   
253  $\text{cm}^{-1}$  having medium or weak intensity.  $PbAs_2O_4$  and  $Pb_2(AsO_2)_3Cl$  show bands of higher  
254 intensity than paulmooreite in the  $660 - 480\text{ cm}^{-1}$  region. The next group of bands which the  
255 dimeric/polymeric arsenites have in common is located in the  $450 - 250\text{ cm}^{-1}$  region.

256

257 Bands in the  $850 - 700 \text{ cm}^{-1}$  region in the spectrum of paulmooreite are assigned to terminal  
258 As-O stretches since these bands are found in the spectra of all of the above lead arsenite  
259 compounds, including finnemanite which does not contain bridging O atoms. Single crystal  
260 data show two  $B_g$  bands at  $760$  and  $755 \text{ cm}^{-1}$ , and two  $A_g$  bands at  $750$  and  $733 \text{ cm}^{-1}$ . HF  
261 calculated data on an isolated  $[\text{As}_2\text{O}_5]^{4-}$  ion presented in a study by Tossell (1997) assigned  
262 terminal O stretches to bands at  $751$ ,  $740$ ,  $739$  and  $734 \text{ cm}^{-1}$  which agrees closely to the  
263 experimental data and HF calculated data of this study which showed bands at  $736$ ,  $720$ ,  $710$ ,  
264 and  $703 \text{ cm}^{-1}$ . Factor group analysis (FGA) on an isolated  $[\text{As}_2\text{O}_5]^{4-}$  ion predicts that each of  
265 these bands (which should possess  $A_1$ ,  $A_2$ ,  $B_1$  and  $B_2$  symmetry) is split into  $A_g$  and  $B_g$   
266 components but the observed number of bands is rather less than that predicted, possibly due  
267 to accidental degeneracies arising from the highly similar terminal bond lengths of the two  
268 inequivalent As atoms.

269

270 Bands in the  $660 - 480 \text{ cm}^{-1}$  region are more intense in the spectra of  $\text{PbAs}_2\text{O}_4$  and  
271  $\text{Pb}_2(\text{AsO}_2)_3\text{Cl}$ , which contain two As-O<sub>b</sub> bonds to one As-O<sub>t</sub>, than in the spectrum of  
272 paulmooreite which contains one As-O<sub>b</sub> and two As-O<sub>t</sub> bonds. The above observation  
273 suggests that this region corresponds to various stretching vibrations of the bridging O atoms.  
274 The spectrum of paulmooreite shows two bands at  $562$  ( $B_g$ ) and  $503 \text{ cm}^{-1}$  ( $B_g$ ). The HF data  
275 of Tossell (1997) showed bridging As-O-As stretches at  $554$  and  $496 \text{ cm}^{-1}$ , in excellent  
276 agreement with the experimental data. The HF data in this study calculated Raman bands  
277 corresponding to the symmetric and antisymmetric bridging O stretches at  $538$  and  $521 \text{ cm}^{-1}$ ,  
278 which also supports the above assignments. FGA on an isolated  $[\text{As}_2\text{O}_5]^{4-}$  ion predicts  
279 stretches of the bridging O giving bands of  $A_1$  and  $B_2$  symmetry; thus it is reasonable to  
280 assign each of the calculated bands to either  $A_1$  or  $B_2$ . Even though there should be an  $A_g$  and

281  $B_g$  component to each of the above modes, the  $A_g$  components in this region may be too weak  
282 to be observed. Though it may be an orientation effect, the  $A_g$  band might be stronger if we  
283 had measured the spectrum in an alternate orientation that wasn't available owing to  
284 birefringence on the b axis.

285

286 The observation that the terminal As-O stretch occurs at a higher wavenumber fits in well  
287 with the shorter terminal As-O bond lengths (ranging from 1.733 to 1.772 Å) compared to the  
288 bridging As-O bond length (1.826 and 1.842 Å). Between vibrations of terminal and  
289 bridging O, there are three bands at 658, 635, and 613  $\text{cm}^{-1}$  in the spectra of paulmooreite that  
290 have not been accounted for. They were not observed in the calculated data for the isolated  
291  $[\text{As}_2\text{O}_5]^{4-}$  ion, indicating the unlikelihood that these bands correspond to As-O vibrations.  
292 Bands of similar appearance and intensity, however, are observed in the spectrum of  
293  $\text{PbAs}_2\text{O}_4$ , which makes it possible that these bands correspond to Pb-O vibrations.

294

295 The next group of bands which dimeric/polymeric lead arsenites have in common occurs at  
296 460 – 240  $\text{cm}^{-1}$ . Bands around 380  $\text{cm}^{-1}$  have been associated with deformations of the As-O-  
297 As unit (Tossell, 1997; Tossell and Zimmermann, 2008; Gout *et al.*, 1997; Pokrovski *et al.*,  
298 1996), and the HF data in this study calculated Raman bands corresponding to deformations  
299 of the terminal O atoms to occur at 386 – 382  $\text{cm}^{-1}$ , and deformations of the bridging O atoms  
300 (although some coupling occurs with the terminal O) at 324 – 318  $\text{cm}^{-1}$ . The spectra of  
301 paulmooreite exhibit  $2A_g + 3B_g$  bands at 383 – 268  $\text{cm}^{-1}$  and  $2A_g + 2B_g$  bands at 460 – 409  
302  $\text{cm}^{-1}$ ; the former region assigned to deformations of the terminal O and the latter to  
303 deformations of the bridging O. Except for the presence of an extra  $B_g$  band in the former  
304 region, the above observation follows the expectation that each calculated band should split  
305 into two components ( $A_g$  and  $B_g$ ) caused by the lower symmetry. Similar to the previous

306 region, bands in this region have a higher intensity in the spectrum of  $\text{PbAs}_2\text{O}_4$  compared to  
307 the other lead arsenites.

308

309 It is difficult to determine whether the experimental Raman spectrum reflects that predicted  
310 by factor group analysis. The low site symmetry caused by the  $90^\circ$  orientation of the  $\text{AsO}_3$   
311 units in the  $[\text{As}_2\text{O}_5]^{4-}$  ion converts all vibrational modes to  $A$  modes and thus the experimental  
312 Raman spectrum only reflects the crystal symmetry. Furthermore it is also difficult to  
313 accurately model and calculate the Raman spectrum of the arsenite ion since its conformation  
314 in paulmooreite is not at an energy minimum in the free ion.

315

316

317 The Raman spectra of synthetic and natural paulmooreite are characterised by three medium  
318 bands at  $800 - 700 \text{ cm}^{-1}$ , weak-medium bands near  $650, 430, 410, 365,$  and  $310 \text{ cm}^{-1}$ , and  
319 strong bands near  $190$  and  $140 \text{ cm}^{-1}$ . The single crystal data of both natural and synthetic also  
320 compare favourably. It is difficult to make band assignments based on symmetry alone due  
321 to the low site symmetry. Spectral comparison with lead arsenites such as synthetic  $\text{PbAs}_2\text{O}_4$   
322 and  $\text{Pb}_2(\text{AsO}_2)_3\text{Cl}$  and natural finnemanite suggests bands at  $760, 755, 750,$  and  $733 \text{ cm}^{-1}$  in  
323 the spectra of paulmooreite correspond to terminal As-O vibrations, whereas stretches of the  
324 bridging O occur at  $562$  and  $503 \text{ cm}^{-1}$ . The assignment above is confirmed by the shorter  
325 terminal As-O bond compared to bridging bonds and by the Raman spectrum of an isolated  
326  $[\text{As}_2\text{O}_5]^{4-}$  ion calculated by HF methods. Factor group analysis predicted  $27A_g + 27B_g$  modes  
327 in the Raman spectrum and in this study  $11A_g + 16B_g$  modes were observed.

328

329

330

331 **REFERENCES**

- 332 Cejka, J., Bahfenne, S., Frost, R. L. and Sejkora, J. (2010) Raman spectroscopic study of the  
333 arsenite mineral vajdakite  $[(\text{Mo}^{6+}\text{O}_2)_2(\text{H}_2\text{O})_2\text{As}^{3+}_2\text{O}_5]\cdot\text{H}_2\text{O}$ . *Journal of Raman Spectroscopy*,  
334 41, 74 – 77.
- 335
- 336 Dinterer, F., Effenberger, H., Kugler, A., Pertlik, F., Spindler, P. and Wildner, M. (1988)  
337 Structure of lead (II) arsenate (III). *Acta Crystallographica*, C44, 2043 – 2045.
- 338
- 339 Dunn, P. J., Peacor, D. R. and Darko Sturman, B. (1979) Paulmooreite, a new lead arsenite  
340 mineral from Langban, Sweden. *American Mineralogist*, 64, 352 – 354.
- 341
- 342 Frisch, M. J. *et al.* (2004) *Gaussian 03, Revision C.02*, Gaussian, Inc., Wallingford, CT
- 343
- 344 Gout, R., Pokrovski, G., Schott, J. and Zwick, A. (1997) Raman spectroscopic study of  
345 arsenic speciation in aqueous solutions up to 275° C. *Journal of Raman Spectroscopy*, 28,  
346 725 – 730.
- 347
- 348 Hirschle, C. and Röhr, C. (2000) Alkalimetall-oxoantimonate: synthesen, kristallstrukturen  
349 und schwingungsspektren von  $\text{ASbO}_2$  (A = K, Rb),  $\text{A}_4\text{Sb}_2\text{O}_5$  (A = K, Rb, Cs) und  $\text{Cs}_3\text{SbO}_4$ .  
350 *Zeitschrift für Anorganische und Allgemeine Chemie*, 626, 1305 – 1312.
- 351
- 352 Klaska, R. and Gebert, W. (1982) Polytypie und struktur von gebhardit –  $\text{Pb}_8\text{OCl}_6(\text{As}_2\text{O}_5)_2$ .  
353 *Zeitschrift für Kristallographie*, 159, 75 – 76.
- 354

355 Moore, P. B., Araki, T. and Brunton, G. D. (1980) Type crystal structure of paulmooreite,  
356  $\text{Pb}_2[\text{As}_2\text{O}_5]$ : dimeric arsenite groups. *American Mineralogist*, 65, 340 – 345.  
357

358 Ondrus, P., Skala, R., Cisarova, I., Veselovsky, F., Fryda, J. and Cejka, J. (2002) Description  
359 and crystal structure of vajdakite,  $[(\text{Mo}^{6+}\text{O}_2)_2(\text{H}_2\text{O})_2\text{As}^{3+}_2\text{O}_5]\cdot\text{H}_2\text{O}$  – A new mineral from  
360 Jachymov, Czech Republic. *American Mineralogist*, 87, 983 – 990.  
361

362 Pertlik, F. (1988) The single chain arsenites  $\text{Pb}(\text{AsO}_2)\text{Cl}$  and  $\text{Pb}_2(\text{AsO}_2)_3\text{Cl}$ . Preparation and  
363 structure investigation. *Zeitschrift für Kristallographie*, 184, 191 – 201.  
364

365 Pertlik, F. and Effenberger, H. (1979) Die Kristallstruktur des Finnemanits,  $\text{Pb}_5\text{Cl}(\text{AsO}_3)_3$ ,  
366 mit einem Vergleich zum Strukturtyp des Chloroapatits,  $\text{Ca}_5\text{Cl}(\text{PO}_4)_3$ . *Tschermaks*  
367 *Mineralogische und Petrographische Mitteilungen*, 26, 95 – 107.  
368

369 Pokrovski, G., Gout, R., Schott, J., Zotov, A. and Harrichoury, J. (1996) Thermodynamic  
370 properties and stoichiometry of As(III) hydroxide complexes at hydrothermal conditions.  
371 *Geochimica et Cosmochimica Acta*, 60, 737 – 749.  
372

373 Tossell, J. A. (1997) Theoretical studies on arsenic oxide and hydroxide species in minerals  
374 and in aqueous solution. *Geochimica et Cosmochimica Acta*, 61, 1613 – 1623.  
375

376 Tossell, J. A. and Zimmermann, M. D. (2008) Calculation of the structures, stabilities, and  
377 vibrational spectra of arsenites, thioarsenites and thioarsenates in aqueous solution.  
378 *Geochimica et Cosmochimica Acta*, 72, 5232 – 5242.  
379



380

381

Band Position (cm <sup>-1</sup> )		Assignment
Natural	Synthetic	
760	761	Bg
755	755	Bg
750	751	Ag
733	733	Ag
658	658	Bg
635	637	Bg
613	613	Bg
	599	?
562		Bg
503	501	Bg
460		Bg
433	434	Ag
412	411	Ag
409	409	Bg
383	384	Bg
367	364	Ag
	355	?
344	344	Bg
312	312	Bg
310	310	Ag
272	274	Ag
268	270	Bg
219	214	Bg
210	209	Ag
186	186	Ag
142	144	Bg
138	139	Ag
120	120	Bg
108	107	Ag

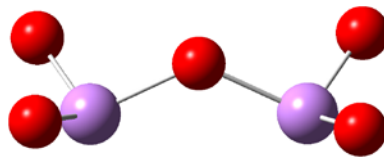
382

383

384 **Table 1 Band symmetry assignments of paulmooreite**

385

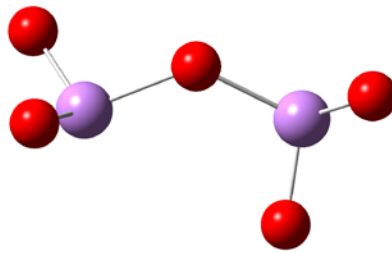
386



387

388

**Fig 1a  $[\text{As}_2\text{O}_5]^{4-}$  dimer in parallel orientation (As:purple)**



389

390

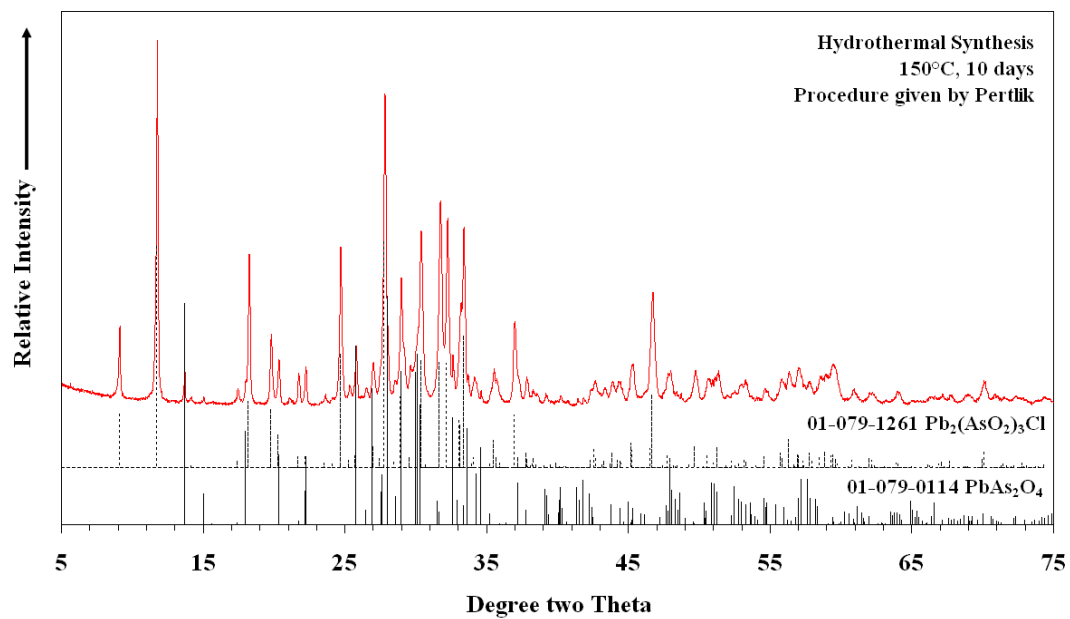
391

**Fig 1b –  $[\text{As}_2\text{O}_5]^{4-}$  dimer in paulmooreite ( $90^\circ$  orientation)**

392

393

394



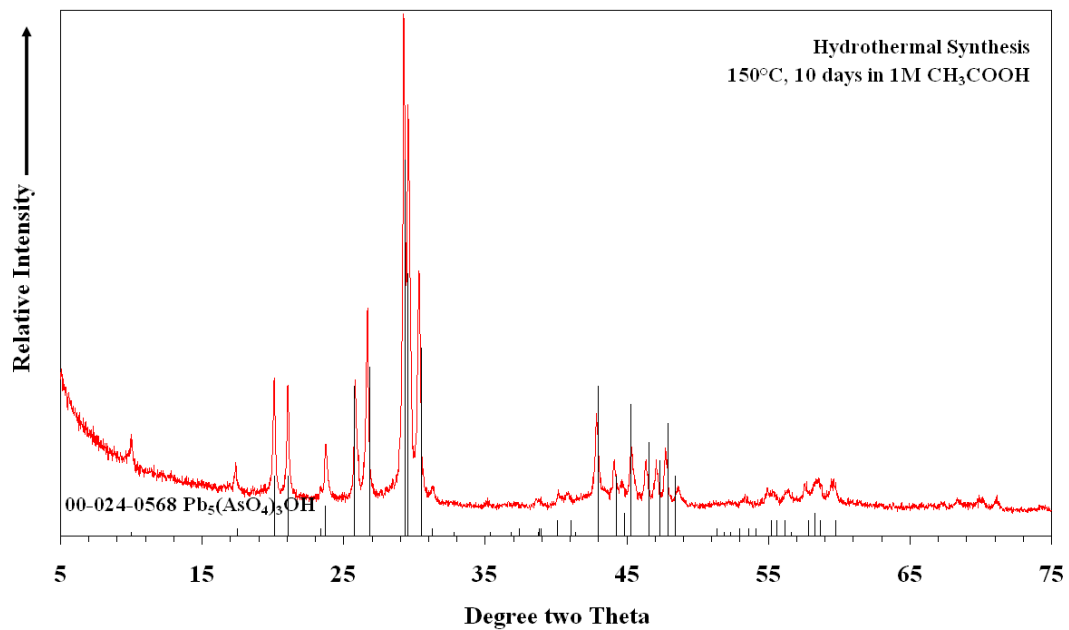
395

396

**Fig. 2 XRD pattern of the product of reaction P3**

397

398



400

401

**Fig. 3 XRD pattern of the product of reaction H1**

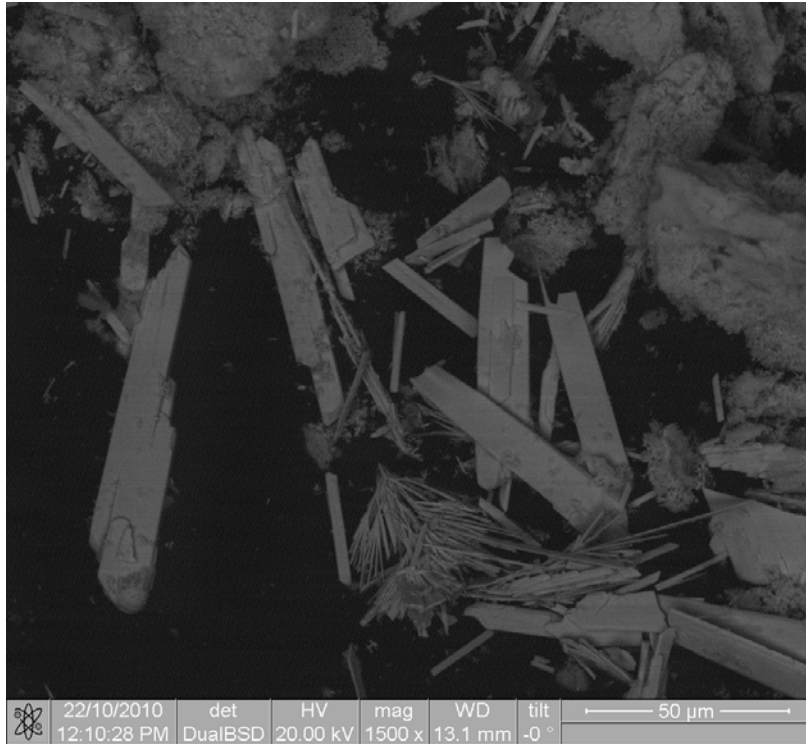
402

403

404

405

406

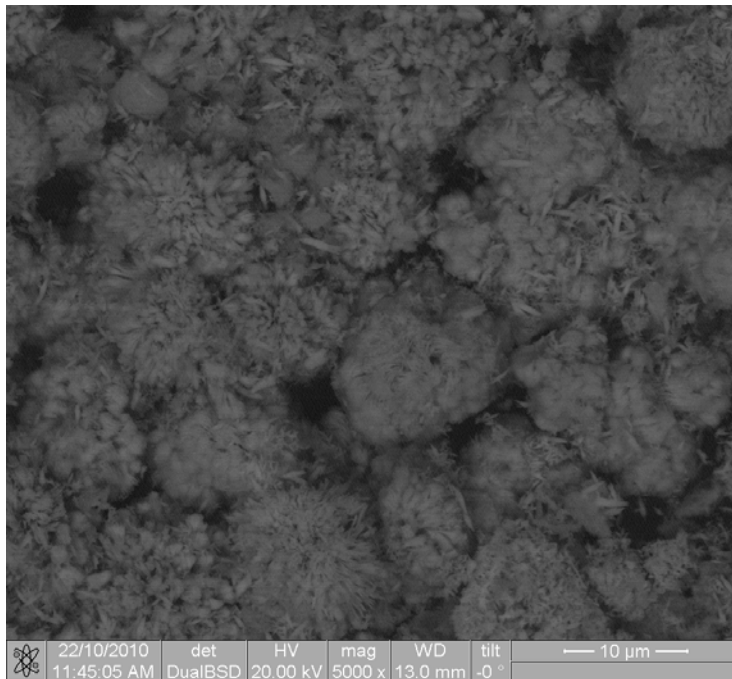


407

408

**Fig. 4a SEM micrograph of product of reaction W1**

409

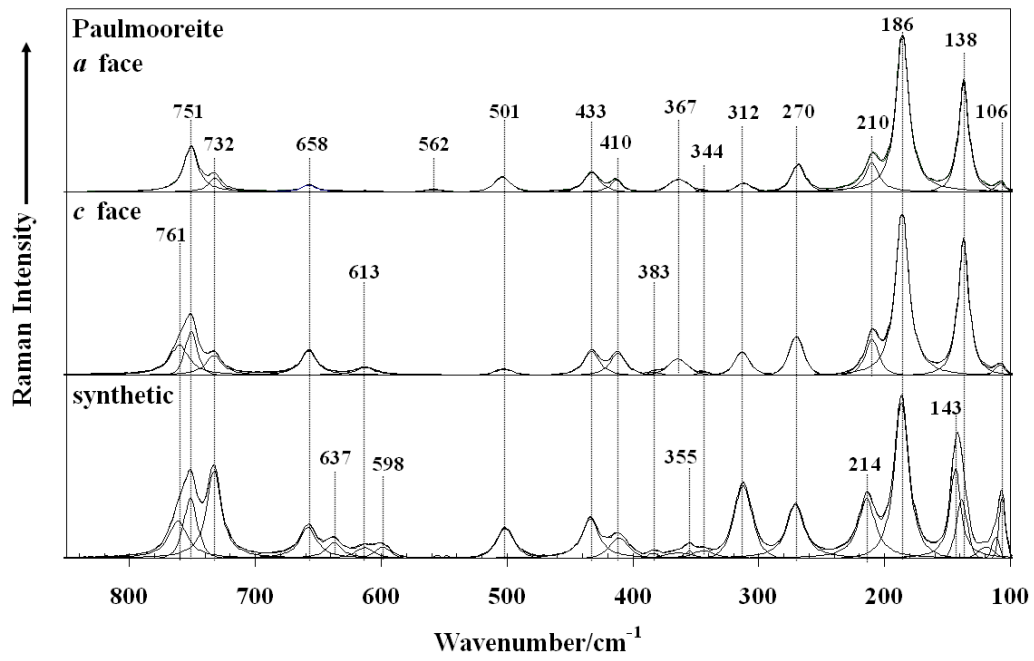


410

411

**Fig. 4b SEM micrograph of product of reaction W2**

412



413

414 **Fig. 5 Raman spectra of natural and synthetic paulmooreite in the 800 – 100 cm<sup>-1</sup> region**

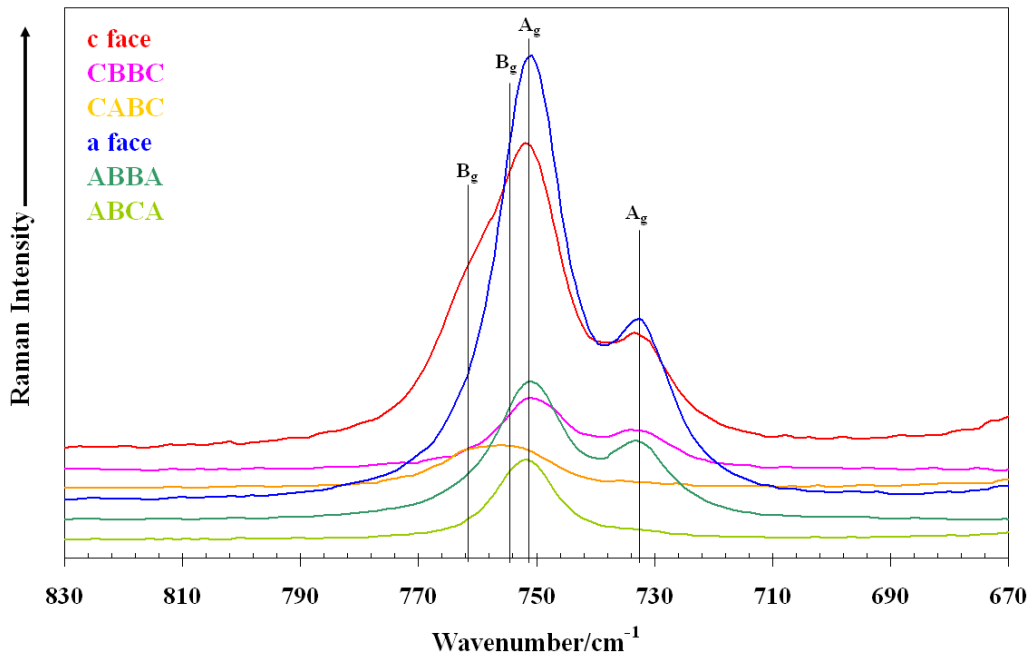
415

416



417

418



419

420 **Fig. 6 Oriented single crystal spectra of natural paulmooreite in the 830 – 670 cm<sup>-1</sup>**

421

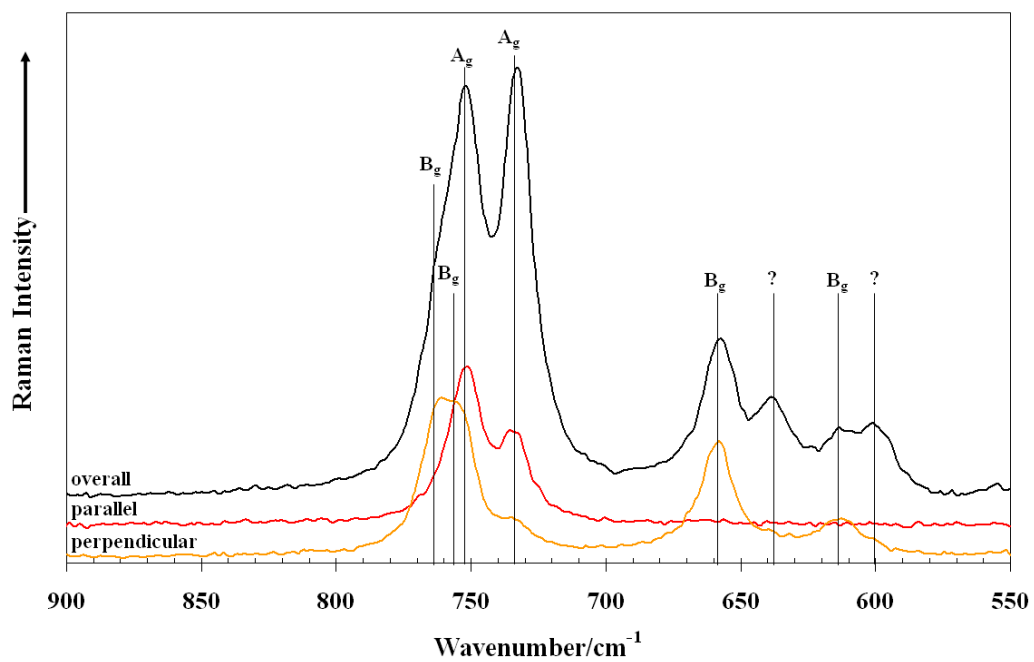
**region**

422

423

424

425



426

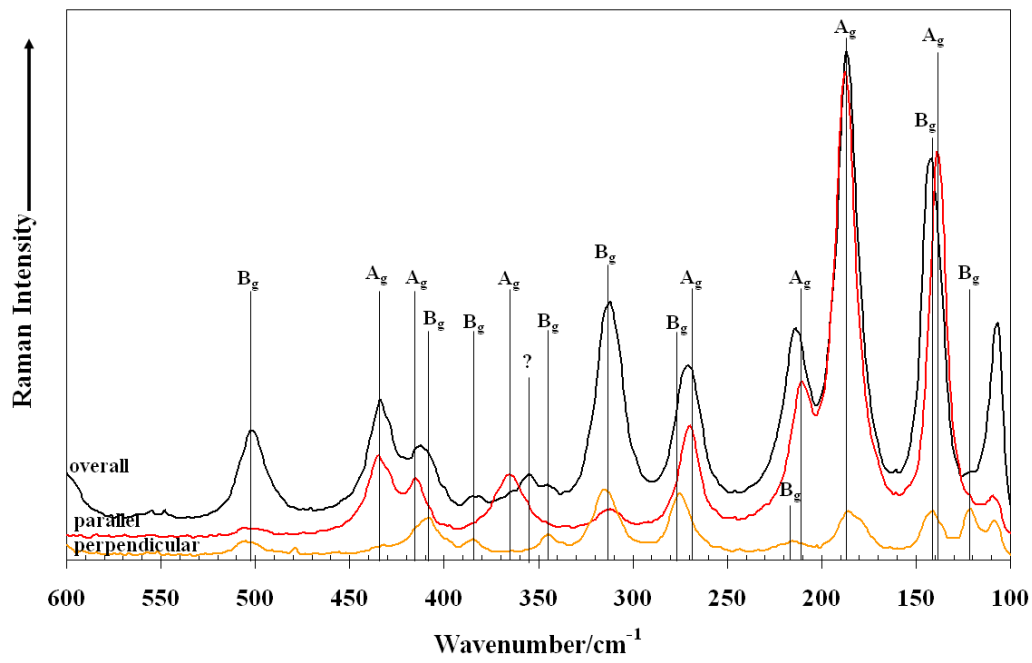
427 **Fig. 7 Oriented single crystal spectra of synthetic paulmooreite in the 900 – 550 cm<sup>-1</sup>**  
428 **region.**

429

430

431

432



433

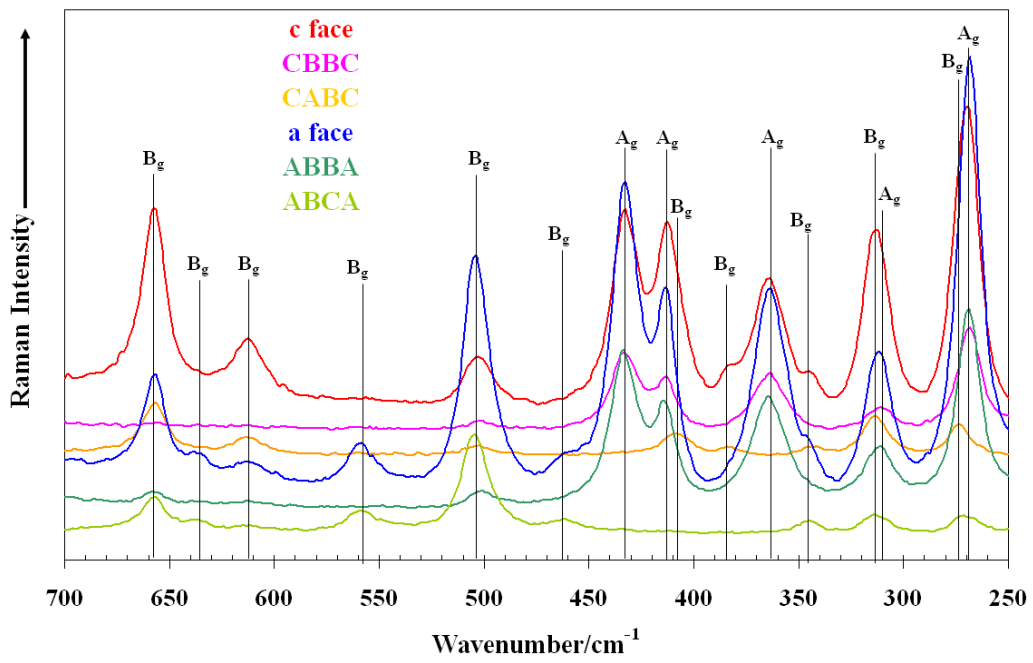
434 **Fig. 8 Oriented single crystal spectra of synthetic paulmooreite in the 600 – 100 cm<sup>-1</sup>**  
435 **region.**

436

437

438

439

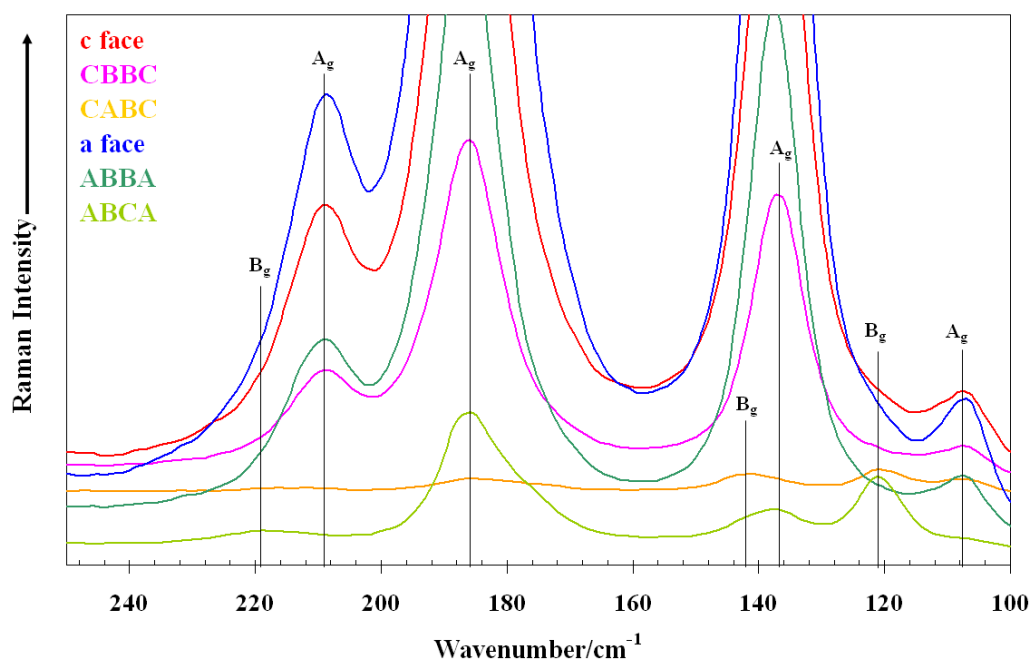


440

441 **Fig. 9 Oriented single crystal spectra of natural paulmooreite in the 700 – 250 cm<sup>-1</sup>**  
442 **region.**

443

444



445

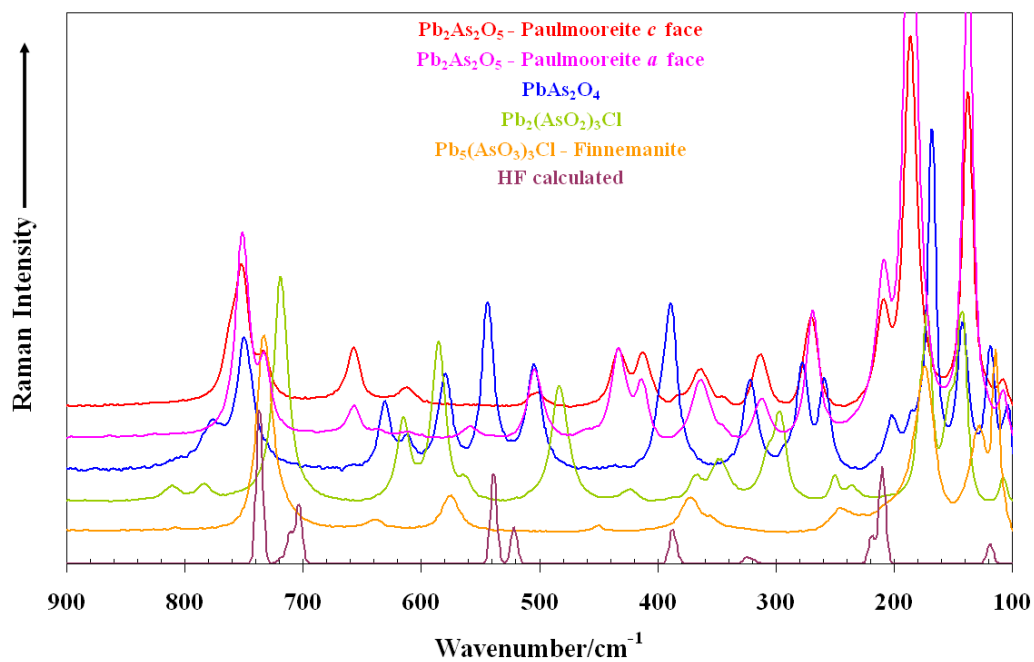
446 **Fig. 10 Oriented single crystal spectra of natural paulmooreite in the 250 – 100 cm<sup>-1</sup>**  
447 **region.**

448

449

450

451



452

453 **Fig. 11 Stacked Raman spectra of paulmooreite,  $Pb_5(AsO_3)_3Cl$ ,  $PbAs_2O_4$ ,  $Pb_2(AsO_2)_3Cl$ ,**  
454 **and HF calculated Raman spectrum of paulmooreite**

455

456

457